Mon. Not. R. Astron. Soc. **000**, 000–000 (0000) Printed 25 June 2020 (MN LATEX style file v2.2)

A β Cepheid, a slowly-pulsating B-star and a changing orbital inclination in the high-mass eclipsing binary system VV Orionis

John Southworth [1], D. M. Bowman [2], K. Pavlovski[3]
[1] *Astrophysics Group, Keele University, Staffordshire, ST5 5BG, UK*
[2] *Institute of Astronomy, KU Leuven, Celestijnenlaan 200D, B-3001 Leuven, Belgium*
[3] *Department of Physics, Faculty of Science, University of Zagreb, Bijenicka cesta 32, 10000 Zagreb, Croatia*

25 June 2020

ABSTRACT
We present an analysis of the high-mass eclipsing binary system VV Ori based on photometry from the TESS satellite. The primary star (B1 V, 9.5 $\mathrm{M}_{\odot}$) shows β Cephei pulsations and the secondary (B7 V, 3.8 $\mathrm{M}_{\odot}$) is a slowly-pulsating B star. We detect 51 significant oscillation frequencies, including a long series of doublets each separated by approximately the orbital frequency, indicating that the pulsations are tidally perturbed. We analyse the TESS light curve and published radial velocities to determine the physical properties of the system. Both stars are only the second of their pulsation type with a precisely-measured mass. The orbital inclination is currently decreasing, likely due to gravitational interactions with a third body.

Key words: stars: fundamental parameters — stars: binaries: eclipsing — stars: oscillations

1 INTRODUCTION

The study of eclipsing binary systems (EBs) is our primary source of empirical measurments of the masses and radii of normal stars (Andersen 1991; Torres et al. 2010). From light and radial velocity (RV) curves the masses and radii can be determined to high precision and accuracy (reaching 0.2%; see Maxted et al. 2020), then used to check and calibrate theoretical models (e.g. Claret & Torres 2018; Tkachenko et al. 2020) or as distance indicators (e.g. Pietrzyński et al. 2019). Massive EBs are of particular interest because massive stars (initial masses $\gtrsim$8 $\mathrm{M}_{\odot}$) have high multiplicity (Sana et al. 2012) and are important drivers in the chemical and dynamical evolution of galaxies (Langer 2012). However, a detailed understanding of their interior rotation and angular momentum transport mechanisms remains elusive (Aerts et al. 2019).

Another method to constrain the properties of massive stars is via asteroseismology (Aerts et al. 2010). Each pulsation mode in a star is sensitive to a specific pulsation cavity, so multi-periodic pulsations are excellent tracers of the properties of stellar interiors (e.g. Aerts et al. 2003; Briquet et al. 2007, 2013). Two classes of massive pulsators are the β Cephei stars (Lesh & Aizenman 1978) and the slowly-pulsating B-type (SPB) stars (Waelkens 1991). The pulsations in β Cep stars are gravity (g) and pressure (p) modes of low radial order, are found in dwarfs and giants of mass 8–15 $\mathrm{M}_{\odot}$, and have amplitudes up to a few tenths of a magnitude and pulsation periods of approximately 2 to 6 hr (Stankov & Handler 2005). SPB stars occur over a mass range of roughly 3–9 $\mathrm{M}_{\odot}$ and are high-order g-modes with observationally-challenging periods of 1 to 4 d. More recently, modern space missions have revealed p- and g-mode pulsations in many massive stars above their canonical mass regimes, and demonstrated the diverse nature of variability for early-type stars (Pedersen et al. 2019; Burssens et al. 2020).

A promising avenue for constraining the interior physics in massive stars is to study pulsating stars in EBs, as this permits the confrontation of theoretical predictions with observed pulsation periods for stars of known mass and radius. Although several β Cep stars in EBs are known (see Ratajczak et al. 2017), so far only one has a precisely-measured mass and radius: V453 Cyg (Southworth et al. 2020). SPB stars in EBs are even rarer: only one has been characterised in detail (V539 Ara; Clausen 1996) and no other examples are known. An important characteristic of binary stars is that tidal effects in eccentric systems may drive (Welsh et al. 2011; Hambleton et al. 2013; Fuller 2017) or perturb (Bowman et al. 2019; Handler et al. 2020; Kurtz et al. 2020) pulsations.

In this work we present an analysis of the high-mass B-type EB VV Orionis (HD 36695) which reveals that the primary star shows β Cep pulsations, the secondary is an SPB star, and the system is undergoing orbital evolution manifested as a changing orbital inclination. VV Ori contains components of spectral types B1 V and B7 V in a circular orbit of period 1.485 d. Its eclipsing nature was discovered by Barr in 1903 (Barr 1905) and the early history of its study has been summarised by Wood (1946) and Duerbeck (1975). The two most recent studies of the system, Sarma & Vivekananda Rao (1995) and Terrell et al. (2007, hereafter T07), were the first to reliably determine its physical properties.

The multiplicity of the VV Ori system is not well established. The excess scatter seen in early RVs led to reluctant suggestions of a third body with an orbital period of 120 d (Daniel 1916; Struve & Luyten 1949), a finding that has not been substantiated (T07, Van Hamme & Wilson 2007). A significant advance has been made by Horch et al. (2017), who resolved a companion at an angular separation of 0.23″ using speckle interferometry. The magnitude differences between this companion and the binary system are 3.88 mag

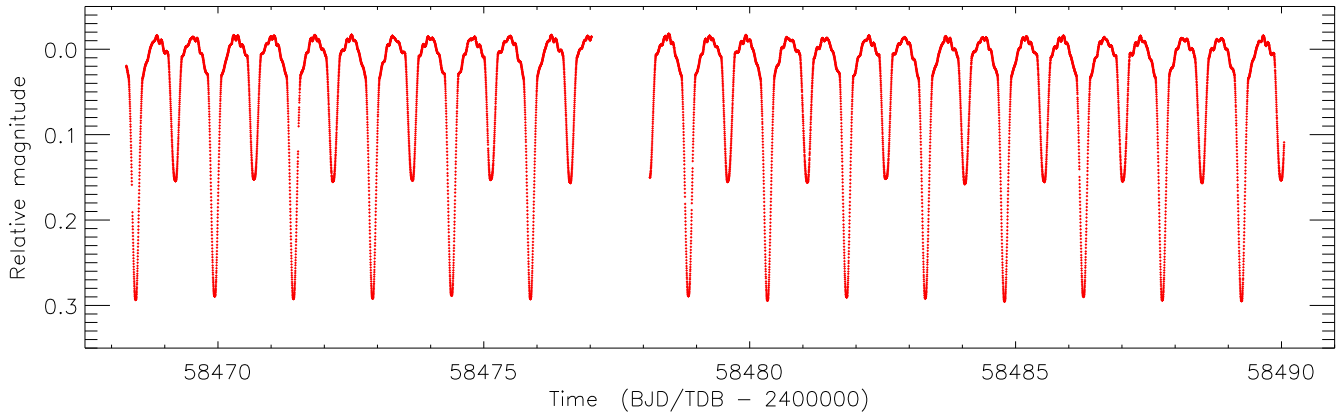

Figure 1. TESS simple aperture photometry (SAP) light curve of VV Ori.

at 692 nm and 3.43 mag at 880 nm (no unertainties quoted). At a distance of 377 ± 31 pc (Gaia Collaboration et al. 2018) this corresponds to a physical separation of 87 au and thus a minimum orbital period of about 180 yr. The resolved companion cannot therefore be responsible for the putative 120 d orbital variations.

2 OBSERVATIONS

VV Ori was observed using the NASA TESS satellite (Ricker et al. 2015). TESS is in the process of observing the majority of the sky, with each hemisphere divided up into 13 sectors based on ecliptic longitude. Observations in each sector last for 27.4 d, with an interruption for data download near the midpoint.

VV Ori was observed in Sector 6 (2018/12/11 to 2019/01/07) and is scheduled to be re-observed in Sector 32 (2020/11/19 to 2020/12/17). The Sector 6 data were acquired at a cadence of 2 min and made available through the MAST portal. Fig. 1 shows the simple aperture photometry light curve (Jenkins et al. 2016) of VV Ori.

3 LIGHT CURVE ANALYSIS

The TESS light curve of VV Ori was first modelled using the JKTEBOP code (see Southworth 2013, and references therein). This code approximates the stars as spheres for the calculation of eclipse light curves: it is fast and provides a good fit but the fitted parameters are unreliable for stars as distorted as the primary star. We used this code to remove the effects of binarity in the light curve, leaving behind residuals containing the pulsation signatures produced by the stars. We used the JKTEBOP fit to normalise the light curve to zero differential magnitude, convert to orbital phase, and bin into 300 datapoints equally spaced in phase.

Because VV Ori A is significantly tidally distorted, we turned to the 2004 version of the Wilson-Devinney code (hereafter WD2004; Wilson & Devinney 1971) for our main light curve analysis, driven by the JKTWD wrapper (Southworth et al. 2011). WD2004 represents the stars using Roche geometry so can accurately model distorted stars but requires much more calculation time. We therefore fitted the phase-binned data obtained from the analysis with JKTEBOP. We fitted separately for the light produced by the two stars, the "third light" from additional star(s) in the system, the potentials of the two eclipsing stars and the orbital inclination. We did not fit for the effective temperatures ($T_{\rm eff}$ values) directly because the TESS passband is not implemented in the WD code. Limb darkening was included using the square-root law, with coefficients fixed to values from the tables of Van Hamme (1993). Fitting for the coefficients did not improve the quality of the fit. We searched for the possibility of an eccentric orbit but found no combination of eccentricity or argument of periastron that improved the fit compared to the assumption of a circular orbit.

The adopted model is given in Table 1 and plotted in Fig. 2, where the residuals come primarily from incomplete removal of the pulsations. Because the Poisson noise in the photometry is negligible, the uncertainties in the fitted parameters are dominated by choices made in the modelling process. We sought to capture these by quantifying the change in fitted parameter values between the adopted model and a range of alternative models with different values or treatments of albedo, stellar rotation rate, gravity darkening, limb darkening law, limb darkening coefficients, the reflection effect, numerical precision, and mass ratio. All uncertainties in Table 1 are the quadrature addition of the differences in parameters for each alternative model versus the adopted model, and are much larger than the formal errors computed by WD2004.

4 PHYSICAL PROPERTIES

Determination of the physical properties of VV Ori requires combining the results of the light curve analysis with spectroscopic measurements of the $T_{\rm eff}$ values and velocity amplitudes (K_1 and K_2) of the two stars. For $T_{\rm eff}$ we adopted the values given by T07 and assigned a conservative uncertainty of $\pm$1000 K. Improved estimates of the $T_{\rm eff}$ values would be helpful in future.

Spectroscopic RV measurements are available from T07, who determined the stellar masses directly and thus did not calculate velocity amplitudes. We therefore fitted the RVs with JKTEBOP to determine $K_1 = 126.2 \pm 1.8$ km s^{-1} and $K_2 = 316.4 \pm 6.5$ km s^{-1}. These uncertainties were calculated using Monte Carlo simulations (Southworth 2008) and with data errors estimated from the scatter around the best fit. Under the assumption that the orbital inclination decreased by $0.200 \pm 0.013^\circ$ yr^{-1} in recent years (see below), K_1 and K_2 should be multiplied by a factor of $(\frac{\sin i_{2018}}{\sin i_{2005}})^3 = 0.979 \pm 0.002$ to correct them from the mean epoch of the spectra to that of the TESS data. The velocity amplitudes at the epoch of the TESS observations are therefore $K_1 = 123.5 \pm 2.0$ km s^{-1} and $K_2 = 309.6 \pm 7.3$ km s^{-1}.

The physical properties of the system were then calculated us-

Table 1. Brief summary of the parameters for the WD solution of the TESS light curve of VV Ori. Detailed descriptions of the control parameters can be found in the WD2004 user guide (Wilson & Van Hamme 2004). Uncertainties are only quoted when they have been robustly assessed by comparison of a full set of alternative solutions.

Parameter	Star A	Star B
Control parameters:		
WD2004 operation mode	0	
Treatment of reflection	1	
Number of reflections	1	
Limb darkening law	3 (square-root)	
Numerical grid size (normal)	60	
Numerical grid size (coarse)	40	
Fixed parameters:		
Orbital period (d)	1.4853784	
Mass ratio	0.376	
Orbital eccentricity	0.0	
Rotation rates	1.0	1.0
Bolometric albedos	1.0	1.0
Gravity darkening	1.0	1.0
Bolometric linear LD coefficients	0.6288	0.7121
Linear LD coefficient	−0.1188	−0.0612
Square-root LD coefficient	0.4694	0.4073
Fitted parameters:		
Orbital inclination (°)	78.28 ± 0.52	
Third light	0.005 ± 0.069	
Light contributions	11.24 ± 0.88	1.299 ± 0.069
Potentials	3.132 ± 0.028	3.397 ± 0.102
Derived parameters:		
Fractional radii	0.3718 ± 0.0010	0.1817 ± 0.0034
Orbital separation ($R_\odot$)	13.51 ± 0.05	
Mass ($M_\odot$)	9.52 ± 0.56	3.80 ± 0.16
Radius ($R_\odot$)	4.958 ± 0.088	2.360 ± 0.061
Log surface gravity (cgs)	4.026 ± 0.011	4.272 ± 0.018
$T_{\rm eff}$ (K)	$26\,200 \pm 1000$	$16\,100 \pm 1000$
Log luminosity ($L_\odot$)	4.017 ± 0.068	2.53 ± 0.11
Absolute bolometric magnitude	-5.36 ± 0.17	-1.65 ± 0.27
Distance (pc)	371 ± 12	

ing the JKTABSDIM code (Southworth et al. 2005), which propagates uncertainties using a perturbation analysis. The distance to the system was calculated from the $UBVRI$ magnitudes from Ducati et al. (2001), assuming an uncertainty of 0.02 mag on each, the JHK_s magnitudes from 2MASS (Skrutskie et al. 2006), and the bolometric corrections from Girardi et al. (2002). An interstellar extinction of $E(B-V) = 0.10 \pm 0.05$ mag was specified to bring the optical and IR distances into agreement. The resulting distance agrees well with the *Gaia* value, which is evidence that the $T_{\rm eff}$ values given by T07 are reliable. We find substantially smaller masses for the two stars than T07, and this can be traced to a significant decrease in the value of K_2 compared to that implied from the masses and orbital period obtained by T07. The uncertainties in both mass and radius are dominated by the contribution from the uncertainty in K_2, and also show that the formal errors from the WD code (quoted by T07) are too small. More extensive spectroscopy of VV Ori is needed to improve its measured properties.

5 ORBITAL EVOLUTION

A small number of EBs have been observed to change their orbital inclinations; this number is growing due to the multitude of photometric surveys that have operated from both ground- and space-based telescopes. The list includes V907 Sco (Lacy et al. 1999), SS Lac (Torres 2001), HS Hya (Zasche & Paschke 2012) and systems discovered using the *Kepler* satellite (Kirk et al. 2016) and the OGLE survey (Soszyński et al. 2016).

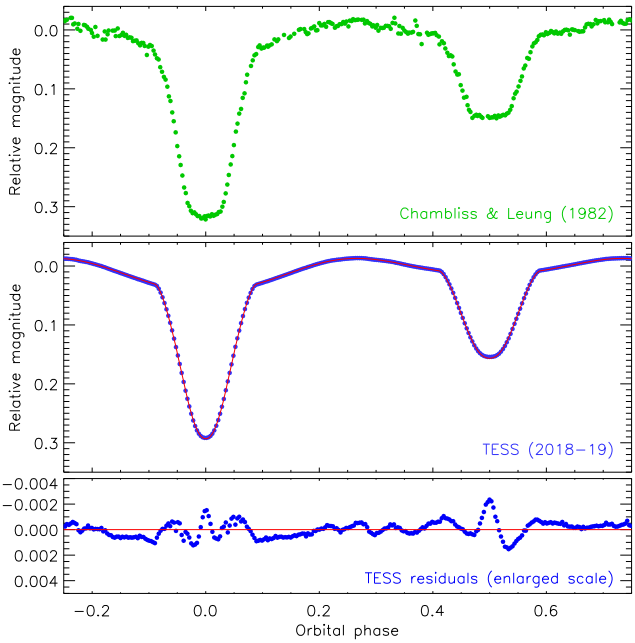

Figure 2. Top: light curve from Chambliss & Leung (1982) obtained by phase-binning the BV and vby data together. Middle: phase-binned light curve of VV Ori (filled blue circles) with the best fit from the WD code (red solid line). Bottom: residuals of the fit to the TESS data.

The TESS light curve of VV Ori shows deep partial eclipses, but previous photometric studies have revealed the system to display obvious total eclipses (e.g. Eaton 1975; Duerbeck 1975; Chambliss & Leung 1982). To demonstrate this we show in Fig. 2 a light curve obtained by phase-binning the data obtained in the Johnson BV filters and the Strömgren vby filters by Chambliss & Leung (1982). The shapes of the two light curves clearly differ. We can rule out a problem with the TESS photometry because a light curve from the MASCARA survey (Burggraaff et al. 2018) shows similar partial eclipses. Our fit to the TESS data gives an orbital inclination of $i = 78.28 \pm 0.52°$, significantly different to the values of $85.9 \pm 0.2°$ found by T07 from the light curve of Chambliss & Leung (1982) and $84.5 \pm 0.5°$ found by Eaton (1975) from his OAO2 data. This suggests that the orbital inclination is changing.

VV Ori benefits from a rich observational history stretching back over a century, but unfortunately none of the early light curves are easily accessible. Investigation of possible changes in i are therefore not trivial. We have found two items of evidence that the inclination was lower in the 1940s. Firstly, Dufay (1947) presents a light curve that shows either partial or marginally total eclipses. His fit to these data, which are rather scattered, gives $i = 77.2°$. Secondly, Huffer & Kopal (1950) state that the period of totality in primary eclipse lasts for 0.042 ± 0.003 phase units. Our by-eye measurement of the duration of totality in the Chambliss & Leung (1982) light curves is 0.060 ± 0.005 in phase units.

Due to the symmetry inherent in spatially-unresolved two-body motion the light curves of EBs have no indication of whether i is above or below 90°, so by convention inclinations are quoted as the smaller of i or $90° - i$. We therefore suggest that VV Ori is

undergoing orbital precession that manifests as a change in i, that it used to show partial eclipses, that the inclination rose to the maximum of $i = 90^\circ$ some time in the 1950s or 1960s, and is now decreasing by approximately 0.2° yr^{-1}. Using WD2004 we find that the lower limit for eclipses to occur in this system is 56.8°. When and if VV Ori will cease to eclipse in the future will be investigated in detail in a future work. One other relevant constraint is that the binarity of the system was discovered through visual observations of its photometic variability in 1903 (Barr 1905). This almost certainly indicates it was eclipsing at this time because the amplitude of the proximity effects in this system is very low for visual observations: roughly 0.04 mag at $i = 60^\circ$.

6 PULSATION ANALYSIS

Owing to the extremely high precision of TESS data, it is practically impossible to achieve a perfect binary-model fit. Therefore, to examine the pulsational properties of VV Ori, we subtracted a multi-frequency harmonic model from the light curve and calculated a residual amplitude spectrum using a discrete Fourier transform (Deeming 1975; Kurtz 1985). We employed iterative prewhitening to extract all significant frequencies using the standard amplitude signal-to-noise (S/N) criterion of Breger (1993), such that significant frequencies have S/N $\geqslant 4$. In total, we extracted 51 significant frequencies between 1.4 and 27.8 d^{-1}. The frequencies, amplitudes and phases, and their corresponding 1σ uncertainties were obtained from a non-linear least-squares fit to the light curve (Kurtz et al. 2015; Bowman 2017), and are provided in Table 2.

Given the masses, $T_{\rm eff}$ values and radii measured for the stars, the primary and secondary components of VV Ori can be classified as β Cep and SPB stars, respectively (Aerts et al. 2010). The TESS light curve of VV Ori reveals a rich pulsation spectrum, with variability in both primary and secondary eclipse. The amplitude spectrum after subtraction of the binary model and our multi-frequency harmonic model is shown in the top panel of Fig. 3, and the corresponding residual amplitude spectrum after all significant pulsation modes have been extracted is shown in the bottom panel.

Our analysis reveals that VV Ori exhibits a long series of frequency doublets, in addition to many other independent pulsation frequencies. These doublets, indicated by vertical blue and red lines in Fig. 3, span a wide frequency range typical of p-modes in β Cep stars, thus likely originate in the distorted primary. Furthermore, the doublets are approximately separated by the orbital frequency of the system, and have an average, yet non-constant, splitting of 0.143 ± 0.002 d^{-1}. The spacing is not the same for each doublet, and on average decreases with increasing frequency. This regularity is clear evidence for the perturbing effect of tides on pulsation mode frequencies in short-period binaries (e.g. Bowman et al. 2019; Southworth et al. 2020). The doublets shown in Fig. 3 are likely rotationlly-split modes in an asynchronous system, as the orbit is circular. Additional 'missing' component frequencies of doublets can clearly be seen in Fig. 3, but these fall below our S/N criterion. Moreover, VV Ori has several independent g- and p-mode pulsation frequencies below 3 d^{-1} and above 10 d^{-1}, respectively. The large number and frequency range of observed pulsations is strong evidence that both stars are pulsating, making VV Ori an excellent target for future binary asteroseismic modelling (see Schmid & Aerts 2016; Johnston et al. 2019).

7 SUMMARY AND DISCUSSION

VV Ori is an early-type binary system containing a 9.5 $\mathrm{M}_\odot$ and 3.8 $\mathrm{M}_\odot$ star on a short-period orbit. It used to show total eclipses but the TESS photometry shows that these eclipses are now partial. We have fitted the TESS light curve and published RVs and determined the physical properties of the stars. The orbital inclination is significantly lower than found in previous studies, and this change is probably driven by dynamical interactions with a third body. Together with the directly-imaged companion at an angular separation of $0.23''$, this means that the VV Ori system is at least quadruple.

The TESS data reveal 51 significant frequencies, including several independent g- and p-mode pulsations below 3 and above 10 d^{-1}, respectively. We interpret the p-mode pulsations as arising from the primary star, making VV Ori A the second β Cephei star in an EB with a precisely measured mass (after V453 Cyg A; see Southworth et al. 2020), and the low-frequency g-mode pulsations to originate from the secondary star, making VV Ori B the second known SPB star in an EB (after V539 Ara B; see Clausen 1996).

A frequency analysis of the TESS light curve also reveals regularity in its frequency spectrum, in the form of a long series of pulsation-mode doublets. Each doublet is approximately separated by the orbital frequency but this spacing, and the spacing between individual frequencies of each doublet, is not constant. The equilibrium tide in short-period circular binaries can not only give rise to a spheroidal bulge and ellipsoidal variability, but is also predicted to perturb self-excited pulsations and produce multiplets of non-radial pulsation frequencies (Reyniers & Smeyers 2003; Balona 2018). Such tidally-perturbed pulsation modes have recently been detected in a handful of short-period EBs (Bowman et al. 2019; Southworth et al. 2020; Jerzykiewicz et al. 2020).

The rich frequency spectrum, which contains a long series of tidally-perturbed modes, makes VV Ori a prime target for furture asteroseismic modelling (see Schmid & Aerts 2016). In the near future VV Ori will be re-observed using TESS, giving a new dataset to further refine the asteroseismic analysis and study the orbital evolution of the system. We have also begun a spectroscopic campaign on this system with the aim of measuring masses and $T_{\rm eff}$ values to higher precision, and detecting line-profile variations due to the pulsations in both components.

ACKNOWLEDGEMENTS

The TESS data presented in this paper were obtained from the Mikulski Archive for Space Telescopes (MAST) at the Space Telescope Science Institute (STScI). STScI is operated by the Association of Universities for Research in Astronomy, Inc. Support to MAST for these data is provided by the NASA Office of Space Science. Funding for the TESS mission is provided by the NASA Explorer Program. The research leading to these results has received funding from the European Research Council (ERC) under the European Union's Horizon 2020 research and innovation programme (grant agreement No. 670519: MAMSIE).

REFERENCES

Aerts, C., Thoul, A., Daszyńska, J., Scuflaire, R., Waelkens, C., Dupret, M. A., Niemczura, E., Noels, A., 2003, Science, 300, 1926

Aerts, C., Christensen-Dalsgaard, J., Kurtz, D. W., 2010, Asteroseismology, Astron. and Astroph. Library, Springer, US

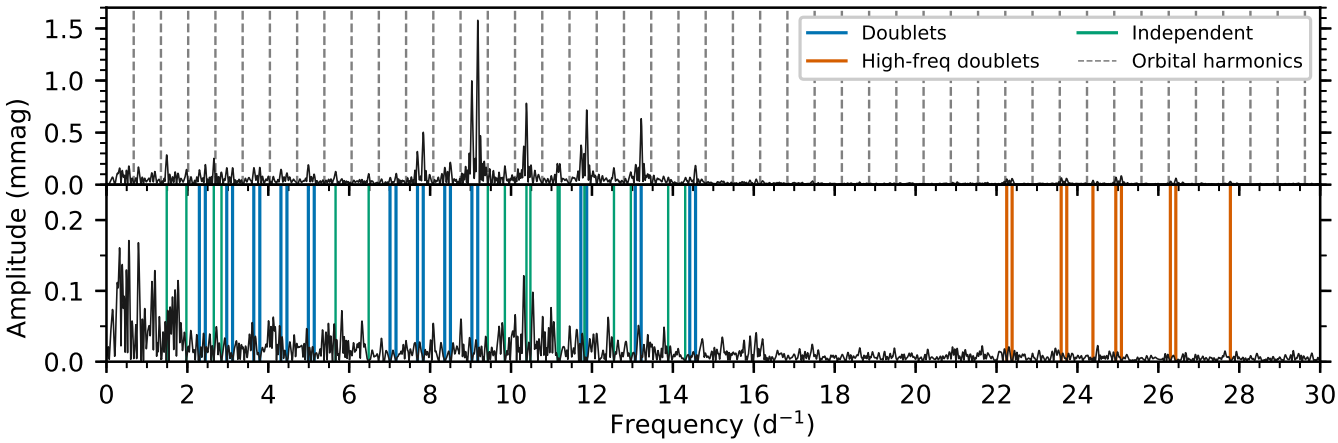

Figure 3. Amplitude spectra of VV Ori after removal of the binary model (top), and after removal of the significant pulsation frequencies too (bottom). The location and identity of extracted frequencies are shown as coloured lines, and the dashed grey lines represent multiples of the orbital frequency.

Aerts, C., Mathis, S., Rogers, T. M., 2019, ARA&A, 57, 35
Andersen, J., 1991, A&ARv, 3, 91
Balona, L. A., 2018, MNRAS, 476, 4840
Barr, J. M., 1905, Selected Papers and Proc. Royal Astron. Soc. of Canada, 42
Bowman, D. M., 2017, Amplitude modulation of pulsation modes in delta Scuti stars, Springer Theses series, Springer, US
Bowman, D. M., Johnston, C., Tkachenko, A., Mkrtichian, D. E., Gunsriwiwat, K., Aerts, C., 2019, ApJ, 883, L26
Breger, M., 1993, Ap&SS, 210, 173
Briquet, M., Morel, T., Thoul, A., Scuflaire, R., Miglio, A., Montalbán, J., Dupret, M. A., Aerts, C., 2007, MNRAS, 381, 1482
Briquet, M., Neiner, C., Leroy, B., Pápics, P. I., MiMeS Collaboration, 2013, A&A, 557, L16
Burggraaff, O., et al., 2018, A&A, 617, A32
Burssens, S., et al., 2020, A&A, in press, arXiv:2005.09658
Chambliss, C. R., Leung, K. C., 1982, ApJS, 49, 531
Claret, A., Torres, G., 2018, ApJ, 859, 100
Clausen, J. V., 1996, A&A, 308, 151
Daniel, Z., 1916, Publ. Allegheny Obs. Pittsburgh, 3, 179
Deeming, T. J., 1975, Ap&SS, 36, 137
Ducati, J. R., Bevilacqua, C. M., Rembold, S. B., Ribeiro, D., 2001, ApJ, 558, 309
Duerbeck, H. W., 1975, A&AS, 22, 19
Dufay, J., 1947, Annales d'Astrophysique, 10, 158
Eaton, J. A., 1975, ApJ, 197, 379
Fuller, J., 2017, MNRAS, 472, 1538
Gaia Collaboration, et al., 2018, A&A, 616, A1
Girardi, L., Bertelli, G., Bressan, A., Chiosi, C., Groenewegen, M. A. T., Marigo, P., Salasnich, B., Weiss, A., 2002, A&A, 391, 195
Hambleton, K. M., et al., 2013, MNRAS, 434, 925
Handler, G., et al., 2020, Nature Astronomy, in press
Horch, E. P., et al., 2017, AJ, 153, 212
Huffer, C. M., Kopal, Z., 1950, AJ, 55, 171
Jenkins, J. M., et al., 2016, in Proc. SPIE, vol. 9913 of *SPIE Conference Series*, p. 99133E
Jerzykiewicz, M., Pigulski, A., Handler, G., Moffat, A. F. J., Popowicz, A., Wade, G. A., Zwintz, K., Pablo, H., 2020, MNRAS, in press, arXiv:2006.05178
Johnston, C., Tkachenko, A., Aerts, C., Molenberghs, G., Bowman, D. M., Pedersen, M. G., Buysschaert, B., Pápics, P. I., 2019, MNRAS, 482, 1231
Kirk, B., et al., 2016, AJ, 151, 68
Kurtz, D. W., 1985, MNRAS, 213, 773
Kurtz, D. W., Shibahashi, H., Murphy, S. J., Bedding, T. R., Bowman, D. M., 2015, MNRAS, 450, 3015
Kurtz, D. W., et al., 2020, MNRAS, 494, 5118
Lacy, C. H. S., Helt, B. E., Vaz, L. P. R., 1999, AJ, 117, 541
Langer, N., 2012, ARA&A, 50, 107
Lesh, J. R., Aizenman, M. L., 1978, ARA&A, 16, 215
Maxted, P. F. L., et al., 2020, MNRAS, in press, arXiv:2003.09295
Pedersen, M. G., et al., 2019, ApJ, 872, L9
Pietrzyński, G., et al., 2019, Nature, 567, 200
Ratajczak, M., Pigulski, A., Pavlovski, K., 2017, in Zwintz, K., Poretti, E., eds., Second BRITE-Constellation Science Conference: Small Satellites - Big Science, vol. 5, p. 128
Reyniers, K., Smeyers, P., 2003, A&A, 404, 1051
Ricker, G. R., et al., 2015, Journal of Astronomical Telescopes, Instruments, and Systems, 1, 014003
Sana, H., et al., 2012, Science, 337, 444
Sarma, M. B. K., Vivekananda Rao, P., 1995, Journal of Astrophysics and Astronomy, 16, 407
Schmid, V. S., Aerts, C., 2016, A&A, 592, A116
Skrutskie, M. F., et al., 2006, AJ, 131, 1163
Soszyński, I., et al., 2016, AcA, 66, 405
Southworth, J., 2008, MNRAS, 386, 1644
Southworth, J., 2013, A&A, 557, A119
Southworth, J., Maxted, P. F. L., Smalley, B., 2005, A&A, 429, 645
Southworth, J., Bowman, D., Tkachenko, A., Pavlovski, K., 2020, MNRAS, 497, L19
Southworth, J., et al., 2011, MNRAS, 414, 2413
Stankov, A., Handler, G., 2005, ApJS, 158, 193
Struve, O., Luyten, W. J., 1949, ApJ, 110, 160
Terrell, D., Munari, U., Siviero, A., 2007, MNRAS, 374, 530
Tkachenko, A., et al., 2020, A&A, 637, A60
Torres, G., 2001, AJ, 121, 2227
Torres, G., Andersen, J., Giménez, A., 2010, A&ARv, 18, 67
Van Hamme, W., 1993, AJ, 106, 2096
Van Hamme, W., Wilson, R. E., 2007, ApJ, 661, 1129
Waelkens, C., 1991, A&A, 246, 453
Welsh, W. F., et al., 2011, ApJS, 197, 4

Wilson, R. E., Devinney, E. J., 1971, ApJ, 166, 605
Wilson, R. E., Van Hamme, W., 2004, Computing Binary Star Observables (Wilson-Devinney program user guide)
Wood, F. B., 1946, Contr. Princeton Univ. Obs., 21, 1
Zasche, P., Paschke, A., 2012, A&A, 542

Table 2. Frequencies, amplitudes and phases of significant frequencies in VV Ori. The uncertainties were calculated from the multi-frequency non-linear least-squares fit. The splittings of doublets are given in the sense of that frequency minus the frequency immediately preceding it in the table.

Frequency (d^{-1})	Amplitude (mmag)	Phase (rad)	Doublet splitting (d^{-1})
1.4892 ± 0.0005	0.2801 ± 0.0059	2.29 ± 0.04	
1.9752 ± 0.0011	0.1298 ± 0.0060	2.82 ± 0.09	
2.2959 ± 0.0010	0.1437 ± 0.0060	-0.01 ± 0.08	
2.4431 ± 0.0009	0.1768 ± 0.0060	-2.70 ± 0.07	0.1473 ± 0.0014
2.6527 ± 0.0007	0.2348 ± 0.0060	1.63 ± 0.05	
2.8432 ± 0.0013	0.1169 ± 0.0060	3.10 ± 0.10	
2.9729 ± 0.0009	0.1654 ± 0.0060	-1.03 ± 0.07	
3.1166 ± 0.0009	0.1665 ± 0.0060	2.88 ± 0.07	0.1437 ± 0.0013
3.6412 ± 0.0008	0.1836 ± 0.0060	-1.39 ± 0.06	
3.7900 ± 0.0008	0.1896 ± 0.0060	2.08 ± 0.06	0.1488 ± 0.0011
4.3122 ± 0.0009	0.1600 ± 0.0060	-2.09 ± 0.07	
4.4608 ± 0.0011	0.1348 ± 0.0060	1.65 ± 0.09	0.1486 ± 0.0014
4.9900 ± 0.0007	0.2068 ± 0.0060	-2.96 ± 0.06	
5.1355 ± 0.0013	0.1175 ± 0.0060	0.84 ± 0.10	0.1455 ± 0.0015
5.6625 ± 0.0012	0.1209 ± 0.0059	2.91 ± 0.10	
6.4807 ± 0.0014	0.1084 ± 0.0059	-0.56 ± 0.11	
7.0084 ± 0.0019	0.0794 ± 0.0060	1.18 ± 0.15	
7.1566 ± 0.0015	0.0965 ± 0.0060	-1.60 ± 0.12	0.1482 ± 0.0024
7.6877 ± 0.0006	0.2701 ± 0.0060	3.12 ± 0.04	
7.8299 ± 0.0003	0.4650 ± 0.0060	-2.66 ± 0.03	0.1423 ± 0.0006
8.3611 ± 0.0008	0.1836 ± 0.0060	2.58 ± 0.06	
8.5016 ± 0.0006	0.2336 ± 0.0060	0.10 ± 0.05	0.1406 ± 0.0010
9.0324 ± 0.0002	0.8916 ± 0.0060	2.00 ± 0.01	
9.1766 ± 0.0001	1.5141 ± 0.0060	2.37 ± 0.01	0.1443 ± 0.0002
9.4262 ± 0.0015	0.1026 ± 0.0059	-1.99 ± 0.12	
9.8475 ± 0.0012	0.1244 ± 0.0059	-1.11 ± 0.09	
10.3808 ± 0.0002	0.8059 ± 0.0060	-2.75 ± 0.02	
10.4786 ± 0.0009	0.1767 ± 0.0060	-2.18 ± 0.07	
11.1526 ± 0.0011	0.1800 ± 0.0065	-0.61 ± 0.08	
11.1998 ± 0.0012	0.1662 ± 0.0065	0.19 ± 0.08	
11.7255 ± 0.0004	0.4148 ± 0.0061	-0.78 ± 0.03	
11.8697 ± 0.0002	0.7435 ± 0.0062	2.65 ± 0.02	0.1442 ± 0.0005
11.8138 ± 0.0019	0.0983 ± 0.0062	-1.93 ± 0.16	
12.5440 ± 0.0010	0.1553 ± 0.0059	1.97 ± 0.08	
12.9610 ± 0.0016	0.1040 ± 0.0060	2.22 ± 0.12	
13.0710 ± 0.0008	0.2112 ± 0.0060	0.84 ± 0.06	
13.2165 ± 0.0002	0.6663 ± 0.0060	-1.99 ± 0.02	0.1455 ± 0.0008
13.8837 ± 0.0019	0.0779 ± 0.0059	-2.45 ± 0.15	
14.3049 ± 0.0029	0.0560 ± 0.0060	-2.59 ± 0.22	
14.4175 ± 0.0028	0.0572 ± 0.0060	2.10 ± 0.22	
14.5605 ± 0.0008	0.1897 ± 0.0059	-0.08 ± 0.06	0.1430 ± 0.0029
22.2519 ± 0.0025	0.0589 ± 0.0060	0.03 ± 0.20	
22.3853 ± 0.0026	0.0577 ± 0.0060	-2.07 ± 0.20	0.1333 ± 0.0036
23.5977 ± 0.0025	0.0594 ± 0.0060	1.97 ± 0.20	
23.7359 ± 0.0023	0.0644 ± 0.0060	-0.69 ± 0.18	0.1383 ± 0.0034
24.3831 ± 0.0050	0.0291 ± 0.0059	2.32 ± 0.40	
24.9480 ± 0.0021	0.0697 ± 0.0059	2.79 ± 0.17	
25.0870 ± 0.0018	0.0841 ± 0.0059	0.64 ± 0.14	0.1390 ± 0.0028
26.2968 ± 0.0041	0.0359 ± 0.0059	-1.99 ± 0.33	
26.4314 ± 0.0025	0.0604 ± 0.0059	2.48 ± 0.20	0.1346 ± 0.0049
27.7800 ± 0.0052	0.0283 ± 0.0059	$-.11 \pm 0.41$	